



## Research article

## Effects of aspect ratio of multi-walled carbon nanotubes on coal washery waste water treatment

Ahmed Aliyu <sup>a, c, \*</sup>, Ishaq Kariim <sup>b, c</sup>, Saka Ambali Abdulkareem <sup>b, c</sup><sup>a</sup> Department of Chemical Sciences, Federal University Wukari, P.M.B. 1020, Taraba State, Nigeria<sup>b</sup> Department of Chemical Engineering, School of Engineering and Engineering Technology, Federal University of Technology Minna, P.M.B. 65, Minna, Niger State, Nigeria<sup>c</sup> Nanotechnology Research Group, Centre for Genetic Engineering and Biotechnology, Federal University of Technology Minna, P.M.B. 65, Minna, Niger State, Nigeria

## ARTICLE INFO

## Article history:

Received 12 April 2017

Received in revised form

26 June 2017

Accepted 6 July 2017

## Keywords:

Multi-walled carbon nanotubes

Catalytic chemical vapour deposition

Characterization

High resolution transmission electron microscope

Dynamic Light Scattering

Aspect ratio

Coal washery

## ABSTRACT

The dependency of adsorption behaviour on the aspect ratio of multi-walled carbon nanotubes (MWCNTs) has been explored. In this study, effect of growth temperature on yield and aspect ratio of MWCNTs by catalytic chemical vapour deposition (CCVD) method is reported. The result revealed that yield and aspect ratio of synthesised MWCNTs strongly depend on the growth temperature during CCVD operation. The resulting MWCNTs were characterized by High Resolution Transmission Electron Microscope (HRTEM), Dynamic Light Scattering (DLS) and X-ray diffraction (XRD) techniques to determine its diameter, hydrodynamic diameter and crystallinity respectively. Aspect ratio and length of the grown MWCNTs were determined from the HRTEM images with the hydrodynamic diameter using the modified Navier-Stokes and Stokes-Einstein equations. The effect of the prepared MWCNTs dosage were investigated on the Turbidity, Iron (Fe) and Lead (Pb) removal efficiency of coal washery effluent. The MWCNTs with higher length (58.17  $\mu\text{m}$ ) and diameter (71 nm) tend to show high turbidity and Fe removal, while MWCNTs with lower length (38.87  $\mu\text{m}$ ) and diameter (45 nm) tend to show high removal of Pb. Hence, the growth temperature during CCVD operation shows a great influence on the aspect ratio of MWCNTs which determines its area of applications.

© 2017 Elsevier Ltd. All rights reserved.

## 1. Introduction

Water resources pollution has been an increasing global challenge for scientific community. Over the last few decades, this pollution by effluent of coal washery, hydrocarbons and heavy toxic metals as a result of human activities have been under serious investigation in a bid to protect and manage the environmental side effects tied to the prevalence of these pollutants. It is however not strange that continuous exposure to heavy metals with relatively high density and atomic weight such as iron, lead, chromium, cadmium and arsenic even at low level over time may result in bioaccumulation and resulting health consequences in humans ((WHO), 2011; Othman et al., 2017). Due to increase in demand for good drinking and industrial water has necessitated the

enforcement of law in protecting the use and processing of water resources.

For the removal of heavy metals from polluted effluent, synthesis of high efficient adsorbent is of paramount importance. The discovery of carbon nanotubes (CNTs) in 1991 (Iijima, 1991) is an important stepping stone for the nano technological progress considering its wide range of applications in areas of water treatment, composites, energy storage and electronic device (Kariim et al., 2017; Shah and Tali, 2016; Su et al., 2016; Tasis et al., 2006; Yang et al., 2013). Unfortunately, the physicochemical properties and cost of production as hinders some of these applications. Basically, CNTs can be synthesised by arc discharge, laser ablation and chemical vapour deposition (CVD) method (Yang et al., 2016; Maria and Mieno, 2015; Voelskow et al., 2014; Hutchison et al., 2001; Tombros et al., 2008; Tsoufis et al., 2008). Among these methods, CVD appears to be the most promising method for industrial scale production of CNTs due to its simplicity, local cost and good morphology properties (Aliyu et al., 2017; Hayder et al., 2017; Iijima and Ichihashi, 1993).

\* Corresponding author. Department of Chemical Sciences, Federal University Wukari, P.M.B. 1020, Taraba State, Nigeria.

E-mail addresses: [ahmedio4ac@yahoo.com](mailto:ahmedio4ac@yahoo.com), [aliyahmed@fuwukari.edu.ng](mailto:aliyahmed@fuwukari.edu.ng) (A. Aliyu).

In the CVD method, hydrocarbons are decomposed on a metal catalyst at a higher temperature of  $\geq 500$  °C to  $\leq 1000$  °C for a certain period of time in a control system. During this process, the precipitation of carbon on the catalyst particles resulted in the formation of CNTs. Reaction temperature, hydrocarbon flow rate, reaction time, catalyst particle size and carrier gas flow rate are the crucial parameters which affect the morphological structure and also determine the type of CNTs produced (Hayder et al., 2017; Tsoufis et al., 2008). These CNTs produced can be either single-walled (SWCNTs) or multi-walled (MWCNTs) as the case may be (Shah and Tali, 2016; Iijima and Ichihashi, 1993; Iijima, 1991). MWCNTs have been used in a great number of applications and its effectiveness depends on their structural parameters such as diameter, number of walls, length and aspect ratio (Abdulrahman et al., 2017; Iijima and Ichihashi, 1993). These aspect ratios pose the major property of MWCNTs which subsequently determine or limit their area of application (Abdulrahman et al., 2017).

In the present study, the effect of growth temperature on the diameter, length and aspect ratio of MWCNTs produced with Fe-Ni catalyst on kaolin support by CVD method was studied. The diameter and hydrodynamic diameter were investigated using HRTEM and Dynamic Light Scattering technique, while the length and aspect ratio of the MWCNTs were determined by relating the diameter from the HRTEM images with the hydrodynamic diameter from Dynamic Light Scattering using the modified Navier-Stokes and Stokes-Einstein equations. Based on our knowledge, there are limited or no literature reports on the effect of aspect ratio of MWCNTs and its application in coal washery waste water treatment. In view of this, the effect of dosage of MWCNTs at different aspect ratio were investigated on the Turbidity, Iron (Fe) and Lead (Pb) removal efficiency from the coal washery effluent in order to improve the quality of water supply and protect the environment.

## 2. Materials and methods

### 2.1. Materials

The acetylene and Argon gases were sourced from BOC Nigeria and they were of analytical grade with percentage purity of 99.99%. Also, the effluent used was obtained from coal washery pond of coal mine at Akwuke, Enugu State, Nigeria.

### 2.2. Methods

#### 2.2.1. Production of MWCNTs

The effect of synthetic temperature on aspect ratio of MWCNTs growth was performed in a CVD reactor consisting of a glass quartz tube, furnace and temperature controller. The catalyst used, which was thoroughly characterized in earlier studies (Aliyu et al., 2017), had a BET surface area of  $3.76 \text{ m}^2/\text{g}$ , pore volume of  $1.9 \times 10^{-3} \text{ cm}^3/\text{g}$  and pore size of  $0.5986 \text{ nm}$ . The HRTEM of the catalyst also show lattice fringes of  $0.3 \text{ nm}$  with estimated catalyst particle size of  $29\text{--}31 \text{ nm}$  (Aliyu et al., 2017). About  $1.0 \text{ g}$  of the prepared calcined catalyst ( $\text{NiFe}_2\text{O}_4/\text{kaolin}$ ) were weighed and spread in a quartz boat ( $11 \text{ cm} \times 2.6 \text{ cm}$ ) and placed at the centre of the glass quartz tube as shown in Fig. 1. The furnace was heated at  $10$  °C/min while argon (Ar) was flowing over the system at  $30 \text{ mL/min}$  to create an inert environment, removal of contaminants and prevent oxidation of the catalyst during the experiment. After the purging of the system from room temperature to  $700$  °C, the Ar flow rate was adjusted to  $230 \text{ mL/min}$  and  $\text{C}_2\text{H}_2$  was then introduced at flow rate of  $150 \text{ mL/min}$  for reaction period of  $45 \text{ min}$ .

The growth experiment was stopped after  $45 \text{ min}$  by switching

off the  $\text{C}_2\text{H}_2$  gas, while the furnace was allowed to cool down to room temperature under a continuous flow of argon at a flow rate of  $30 \text{ mL/min}$ . The quartz tube was disconnected from the setup and the quartz boat was removed and the CNTs deposit was weighed.

The growth reactions were performed at the following temperatures:  $750$ ,  $800$ ,  $850$  and  $900$  °C. To ensure comparability, the experiments were conducted using the same mass of catalyst ( $1.0 \text{ g}$ ), constant flow rate of argon and acetylene. The investigation of the aspect ratio at different growth temperature was conducted after the characterization of the prepared MWCNTs using HRTEM and Dynamic Light Scattering technique to determine its morphology and hydrodynamic diameter respectively.

#### 2.2.2. Characterization of MWCNT

The grown MWCNTs samples' surface morphology was examined using high resolution transmission electron microscope (Phillips CM20FEG), while the hydrodynamic diameter were determined using Dynamic Light Scattering; Zetasizer (Nano S). For HRTEM studies, the samples were prepared by sonication of MWCNTs in isopropanol and few drops of the resultant suspension was put onto holey copper grid and dried for the analysis. Also, for the Dynamic Light Scattering technique,  $1 \text{ mg}$  of the samples were dispersed in  $10 \text{ mL}$  of an organic solvent (methanol) by means of a sonication (Misonix 3000; power:  $1 \text{ W/mL}$ , pulse on:  $3 \text{ s}$ , pulse off:  $3 \text{ s}$ , time:  $1 \text{ min}$ ) and a centrifugation ( $5 \text{ min}$  @  $3000 \text{ rpm}$ ). The supernatant was then transferred into a polystyrene quartz cuvette using a syringe with  $0.22 \text{ }\mu\text{m}$  filters and placed in the Zetasizer Nano S cuvette holder immediately for analysis. The crystal phase identification of MWCNTs was performed using Bruker AXS D8 X-ray diffractometer system coupled with  $\text{Cu-K}\alpha$  radiation of  $40 \text{ kV}$  and a current of  $40 \text{ mA}$ . The  $\lambda$  for  $\text{K}\alpha$  was  $0.1541 \text{ nm}$ , scanning rate was  $1.5^\circ/\text{min}$ , while a step width of  $0.05^\circ$  was used over the  $2\theta$  range value of  $20\text{--}80^\circ$ .

#### 2.2.3. Coal washery effluent and treatment

The effluent samples from coal washery pond of coal mine at Akwuke, Enugu State, Nigeria were collected and stored in a tight container and its turbidity, Fe and Pb contents were pre-determined before treatment. Jar test analysis was carried out by adding  $200$ ,  $400$ ,  $600$ ,  $800$  and  $1000 \text{ mg}$  of the prepared MWCNTs on  $1000 \text{ mL}$  of coal washery waste water sample and its turbidity were determined using turbidity meter. The turbidity removal percentage of each of the prepared MWCNTs was calculated using Equation (1). While in another set of experiment,  $1000 \text{ mL}$  of the effluent were treated with  $200$ ,  $400$ ,  $600$ ,  $800$ , and  $1000 \text{ mg}$  at  $1000 \text{ rpm}$  stirring speed for  $45 \text{ min}$  and allowed to settle and filter. The filtrates were analysed using the AAS machine to measure the Fe and Pb concentration.

$$\text{Turbidity Removal Efficiency (\%)} = \frac{N_0 - N}{N_0} \times 100 \quad (1)$$

where  $N_0$  and  $N$  are the initial and final turbidity in NTU.

## 3. Results and discussion

The effect of the growth temperatures on the yield of MWCNTs produced was studied under the same reaction conditions: growth times ( $45 \text{ min}$ );  $\text{C}_2\text{H}_2$  flow rate ( $150 \text{ mL/min}$ ) and Ar ( $280 \text{ mL/min}$ ); and the results obtained were presented in Fig. 2. The result shows that as the reaction temperature increased from  $700$  °C to  $750$  °C, the mass quantities of MWCNTs produced increased after which

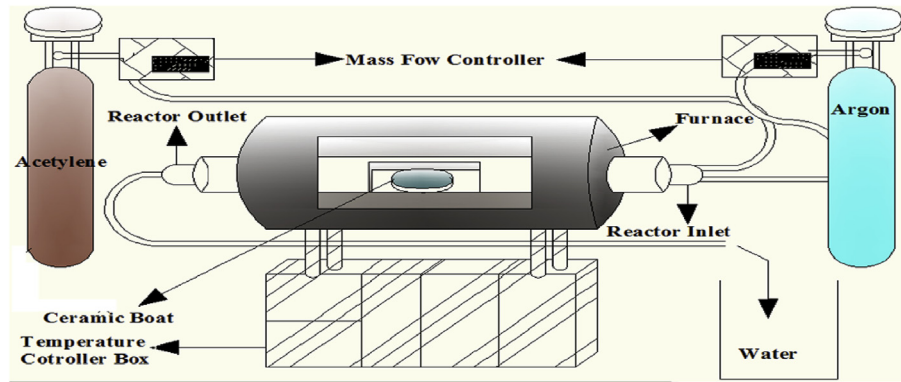


Fig. 1. Diagram of the experimental setup for MWCNTs production (Aliyu et al., 2017).

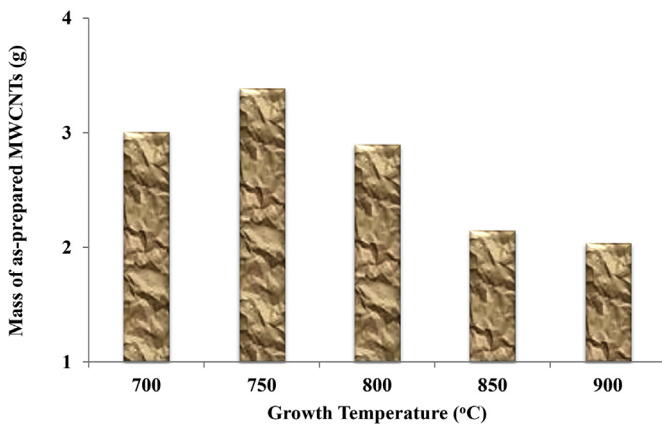


Fig. 2. Effect of growth temperature on the mass of as-produced CNTs.

above 750 °C (i.e. 800, 850 and 900 °C), the quantities of MWCNTs produced decreased. This can be attributed to high decomposition of the  $C_2H_2$  over the catalyst at 750 °C which provides more growth surface for the selectivity of the CNTs formation, while the low mass of MWCNTs production above 750 °C are attributed to low decomposition of the  $C_2H_2$  over the catalyst and the deactivation of the catalyst's pores at elevated temperature.

While the increase in growth temperature negatively affects the masses of CNTs produced (Fig. 2), the reverse is the case on the diameters of the synthesised CNTs. Figs. 3–7(a) shows the HRTEM images of MWCNTs produced over Fe-Ni/kaolin catalyst at 700, 750, 800, 850, and 900 °C growth temperature respectively. The HRTEM images shows a well graphitized wall structure of MWCNTs and little encapsulated catalyst particles without an indication of amorphous carbon on the surfaces of the synthesised MWCNTs. The effect of increasing the growth temperature of the CVD was observed as an increase in the diameter of the MWCNTs produced. The highest MWCNTs diameter was produced at 900 °C relative to those produced at lower temperatures growth. This can be probably attributed to the fact that, at higher temperatures, Fe-Ni active site of the catalyst species merged on the kaolin surface, forming larger catalyst particles that caused to form wider diameter MWCNTs formation by the tip growth (Kukovitsky et al., 2002). Besides, Zhao et al. (2010) suggested possibility of  $C_2H_2$  decomposition on MWCNTs sidewalls, leading to tube diameter thickening.

The significance importance of aspect ratio and the dynamic light scattering (DLS) analysis were used to study the effect of growth temperature on MWCNTs production. Presented in Table 1 is the Z-average (nm) of the prepared MWCNTs at different growth

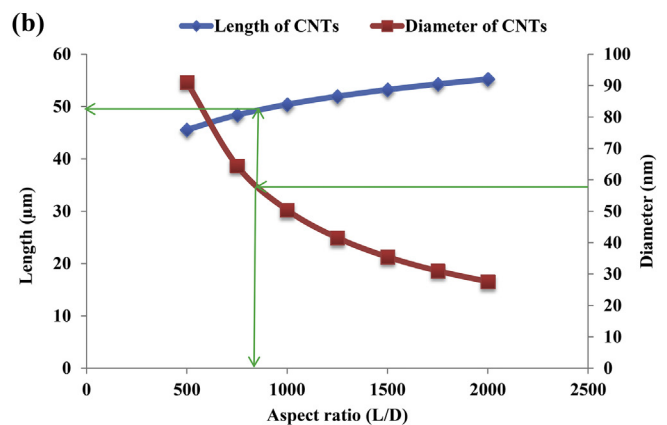
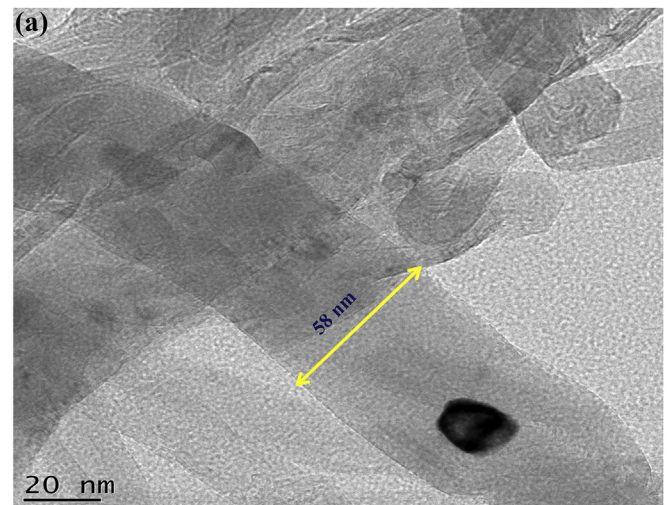


Fig. 3. (a) HRTEM micrograph (b) Aspect ratio correlation of MWCNTs at 700 °C.

temperature from the DLS analysis.

The effect of growth temperature on the aspect ratio (L/D) of MWCNTs was investigated by establishing a DLS-correlation chart. This was achieved by relating the diameter of as-prepared MWCNTs from the HRTEM images with the  $D_h$  (hydrodynamic diameter) using the modified Navier-Stokes and Stokes-Einstein equation in Equations (2) and (3) respectively (Nair et al., 2008). The chart is aimed at determining the aspect ratio and length at a specific diameter of the synthesised MWCNTs.

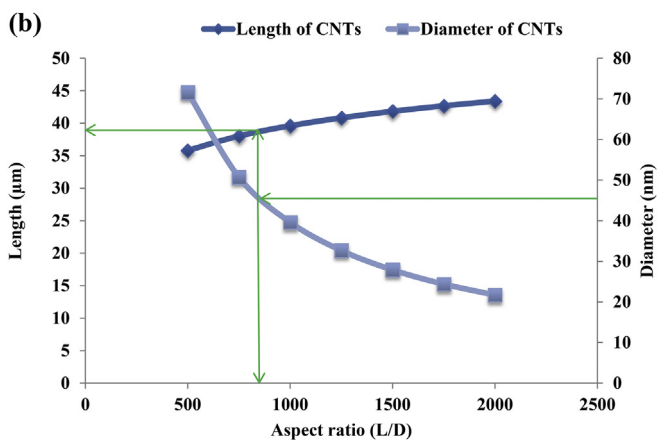
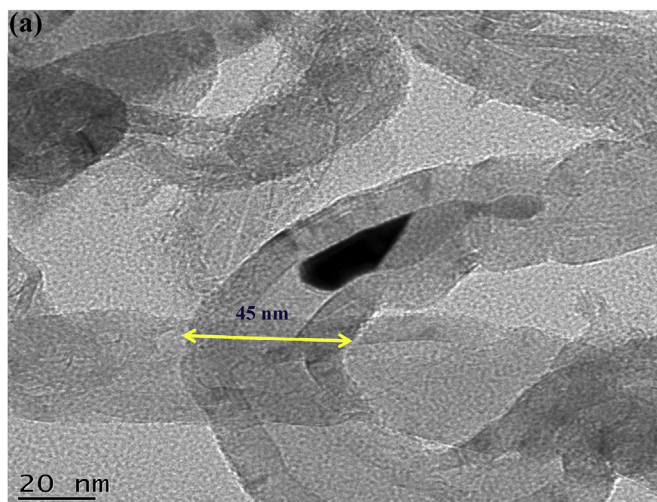


Fig. 4. (b) HRTEM micrograph (b) Aspect ratio correlation of MWCNTs at 750 °C.

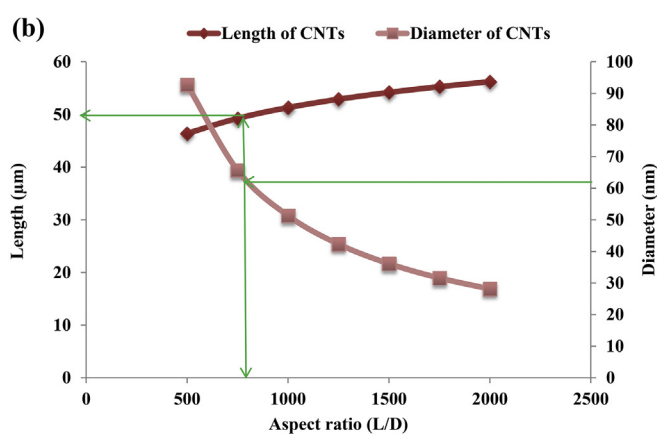
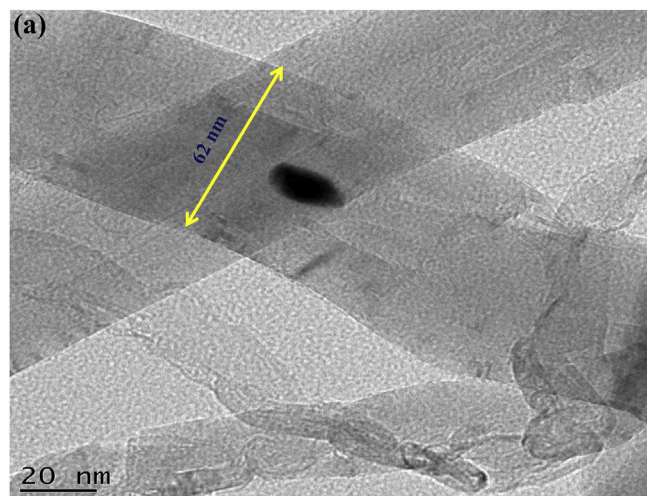


Fig. 5. (a) HRTEM micrograph (b) Aspect ratio correlation of MWCNTs at 800 °C.

$$D = \frac{kT}{3\pi\eta L} \left[ \ln\left(\frac{L}{d}\right) + 0.32 \right] \quad (2)$$

$$D = \frac{kT}{3\pi\eta D_h} \quad (3)$$

where D is the diffusion coefficient, k is the Boltzmann constant, T is temperature, η is the viscosity, D<sub>h</sub> is the hydrodynamic diameter, and “L” and “d” are the length and diameter of the nanotube, respectively. Combining the equations by relating the D<sub>h</sub> to the dimensions of the nanotube in the form of Equation (4):

$$D_h = \frac{L}{\ln\left(\frac{L}{d}\right) + 0.32} \quad (4)$$

From the DLS Zetasizer results presented in Table 1, the hydrodynamic diameters of the prepared MWCNTs at 700, 750, 800, 850 and 900 °C were 6971, 5480, 7098.2, 7890.3 and 8269 nm respectively. The developed correlation charts are presented in Fig. (3)–(7)(b).

From correlation charts in Fig. (3)–(7)(b), the lengths and aspect ratio (L/D) of the prepared MWCNTs were determined and presented in Table 2. It was observed that increasing growth temperature from 700 °C to 750 °C resulted in decrease in length of MWCNTs, but above 750 °C (i.e. 800, 850 and 900 °C) the length were found to increase (See Fig. 8). Moreover, effects of growth

temperature on the aspect ratios were observed to be sinusoidal in patterns as show in Fig. 9. This indicates that the length and aspect ratio of the MWCNTs changes with CVD growth temperature.

The crystallinity of the prepared MWCNTs was characterized via the X-ray diffraction (XRD) techniques. The result of the analysis is presented in Fig. 10. The crystallography of the prepared MWCNTs practically has similar characteristics at the same diffraction angle at 2θ equal 26° and 44°, which correspond to the crystal planes [200] and [100] respectively and they are denoted by letter “C”, represent the characteristic planes of a typical graphitized carbon of the CNTs.

### 3.1. Composition of the coal washery effluent

The prepared MWCNTs at different aspect ratio were used at different dosage for the removal of the turbidity, Fe and Pb ions concentration from coal washery waste water effluent. The initial turbidity, Fe<sup>2+</sup> and Pb<sup>2+</sup> concentration of the sample waste water are 4576 NTU, 4.25 mg/L and 0.16 mg/L respectively at a pH of 3.51.

### 3.2. Effect of MWCNTs dosage of different aspect ratio on turbidity removal of coal washery effluent

The effect of MWCNTs dosage at different aspect ratio on the turbidity removal of coal washery effluent is presented in Fig. 11. These studies showed decrease in the turbidity removal with the increase in the dosage of MWCNTs for all the samples. It is noticed

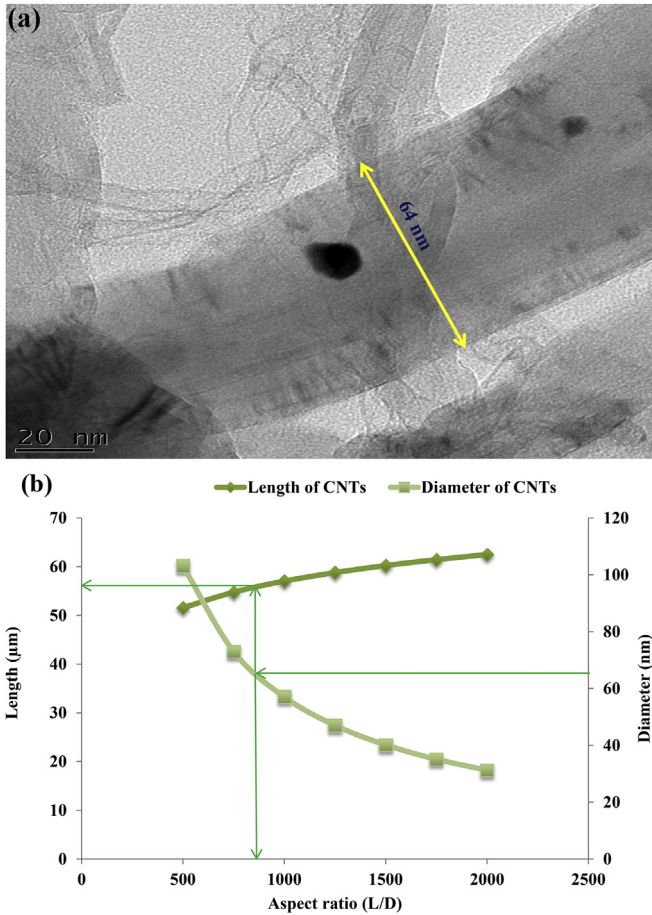


Fig. 6. (a) HRTEM micrograph (b) Aspect ratio correlation of MWCNTs at 850 °C.

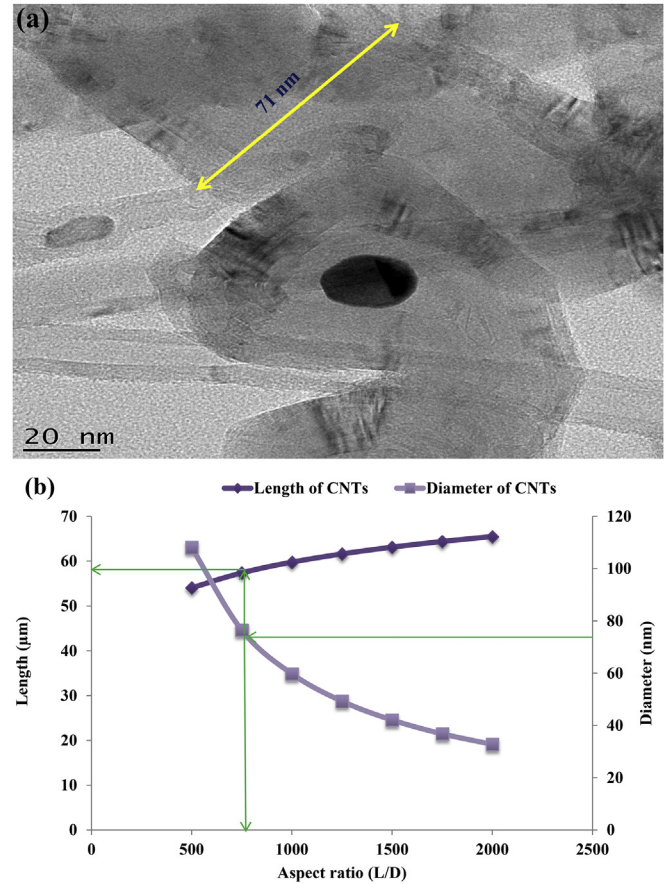


Fig. 7. (a) HRTEM micrograph (b) Aspect ratio correlation of MWCNTs at 900 °C.

from the figures that the highest turbidity removal for the sample was achieved at 400 mg dosage of MWCNTs. The turbidity removal was found to increase from 59.99% (Fig. 11 (b)) to 99.97% (Fig. 11 (e)) as the diameter and length of the MWCNTs increases from 45 nm and 38.84 µm to 71 nm and 58.17 µm respectively. These results show the dependency of turbidity removal in coal washery effluent on the length and diameter (i.e. aspect ratio (L/D)) of MWCNTs. The consistency of these findings was also confirmed on the basis of correlation coefficient values and the results show the highest R<sup>2</sup> value of 90.27% at the optimum turbidity removal of 99.97% in Fig. 11 (e).

3.3. Effect of MWCNTs dosage of different aspect ratio on iron (Fe) and lead (Pb) removal efficiency of coal washery effluent

The bubble plots as depicted in Figs. 12 and 13 show the effect of MWCNTs dosage of different aspect ratio on Iron (Fe) and Lead (Pb) removal efficiency from coal washery effluent respectively. The results show that an increase in MWCNTs dosage increases the removal of Fe and Pb ion concentration from the effluent. The optimum dosage of 1000 mg of MWCNTs was achieved for both heavy metals considered. At the optimum dosage, the removal of Fe from the coal effluent increases from 71.2% (Fig. 12 (b)) to 89.66% (Fig. 12 (e)) as the length and diameter of the MWCNTs increases from 38.84 µm and 45 nm to 58.17 µm and 71 nm respectively. These findings can be attributed to the fact, as the length and diameter of the MWCNT increases, there are more available free active sites areas in the adsorbents which resulted to an increase the effective

Table 1  
Z-average of MWCNTs at different growth temperature.

Growth temperature (°C)	Diameter of CNTs (nm)	Z-average (nm)
700	58	6971.00
750	45	5480.00
800	62	7098.20
850	64	7890.30
900	71	8269.00

surface area for the adsorption of the Fe metals present in the effluent. While on the basis of correlation coefficient values, MWCNTs with the lowest length and diameter tend to show the best satisfactory fit with highest R<sup>2</sup> value of 99.22% (See Fig. 12 (b)).

On the other hand, at the optimum dosage of 100 mg of MWCNTs, the Pb removal efficiency decreases from 95.71% (Fig. 13 (b)) to 67.97% (Fig. 13 (d)) with increase length and diameter of the MWCNTs from 38.84 µm and 45 nm to 56.04 µm and 64 nm respectively. These revealed that for an optimum Pb removal, MWCNTs with small length and diameter will be required. But on the basis of correlation coefficient values, MWCNTs with length and diameter of 56.04 µm and 64 nm respectively tend to show the best satisfactory fit with highest R<sup>2</sup> value of 93.52% (See Fig. 13 (d)). It is important to note that, at the highest length and diameter of 45 nm–58.17 µm and 71 nm respectively, the optimum dosage was found to be 200 mg corresponding to 67.23% Pb removal with correlation coefficient values of 80.70% (See Fig. 13 (e)). This observable variation may be due to collapsing of available free sites for adsorption taking place after a dose of 200 mg. It is evident from the results that, MWCNTs with highest length (58.17 µm) and

**Table 2**  
Aspect ratios and lengths of MWCNTs at different Growth temperature.

Growth temperature (°C)	Diameter of CNTs (nm)	Z-average (nm)	Length of MWCNTs (μm)	Aspect ratio (L/D)
700	58	6971.00	49.30	865.18
750	45	5480.00	38.84	878.57
800	62	7098.20	49.79	814.03
850	64	7890.30	56.04	890.97
900	71	8269.00	58.17	832.34

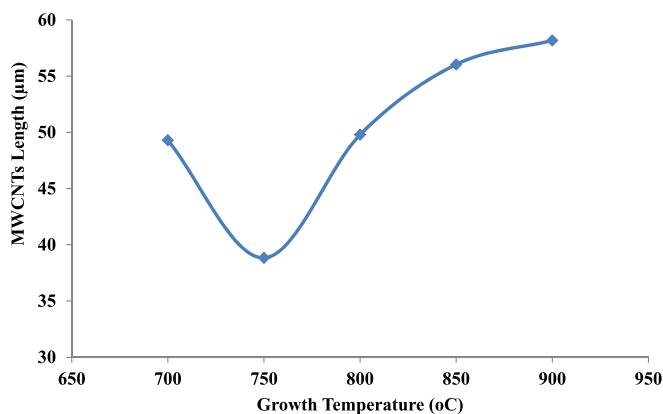


Fig. 8. Effect of Growth temperature on the length of MWCNTs.

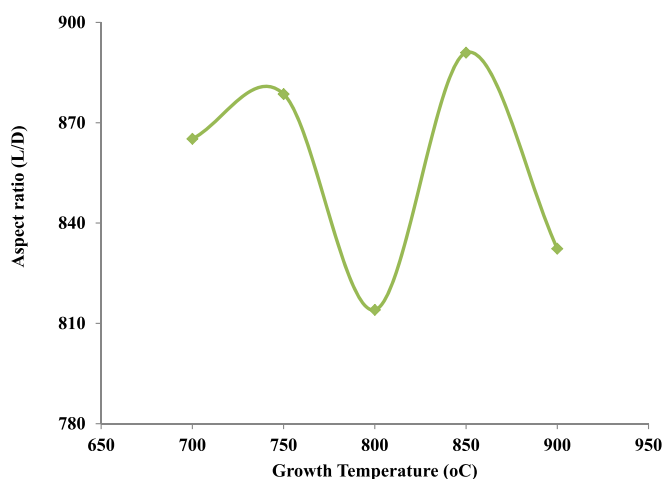


Fig. 9. Effect of Growth temperature on the aspect ratio of MWCNTs.

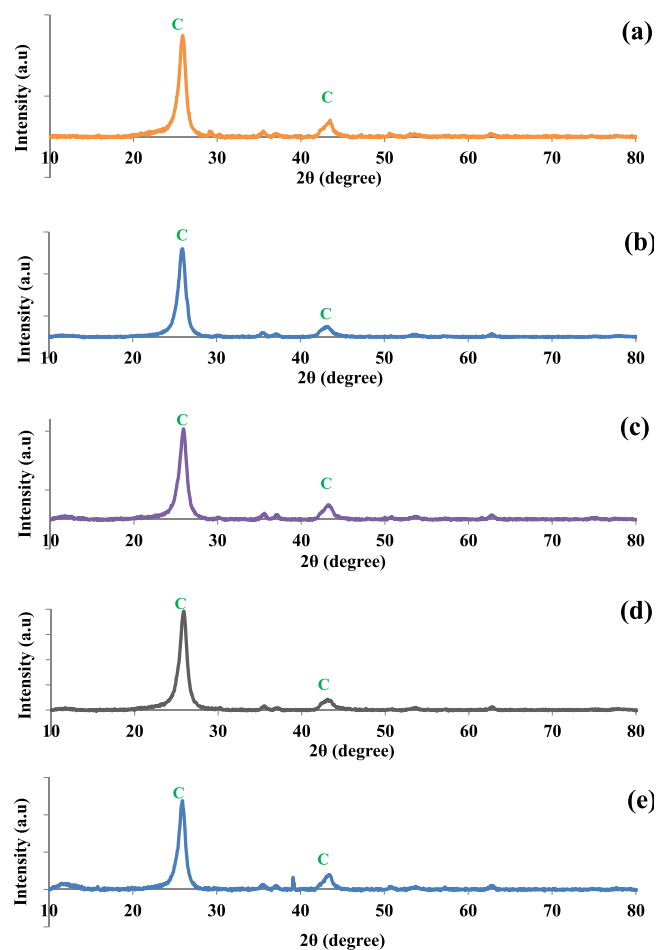


Fig. 10. X-ray diffraction patterns of MWCNTs: (a) 700 °C (b) 750 °C (c) 800 °C (d) 850 °C (e) 900 °C.

diameter (71 nm) tend to show good adsorbing capacity for Fe while MWCNTs with lowest length (38.84 μm) and diameter (45 nm) gives good removal of Pb.

#### 4. Conclusions

In this study, the effect of growth temperature on the yield, diameter, length and aspect ratio of MWCNTs were investigated. The results of the analysis show that increase in growth temperature from 700 to 750 °C resulted in the increase of mass of synthesised MWCNT. While, above 750 °C the mass decreases with respect to growth temperature. Moreover, the HRTEM images revealed formation of well graphitized wall structures of MWCNTs which tube diameter increases with increased in the growth temperature from 750 to 900 °C, while the aspect ratios (L/D) form a

sinusoidal pattern effect with respect to temperature. Furthermore, the XRD results revealed the graphitized carbon nature of the prepared MWCNTs at 2θ angle of 26° and 44° with corresponding crystal planes of [200] and [100] respectively. Also, the highest removal of Fe and Pb was achieved at 1000 mg dosage of the MWCNTs while the highest turbidity removal was achieved at 400 mg dosage. In addition, MWCNTs with highest length (58.17 μm) and diameter (71 nm) tend to show good adsorbing capacity for turbidity and Fe removal while MWCNTs with lowest length (38.84 μm) and diameter (45 nm) gives good removal of Pb. Therefore, this study demonstrated for the first time the dependency of turbidity, Fe and Pb removal of coal washery effluent on the length to diameter (aspect ratio) of the synthesised MWCNTs.

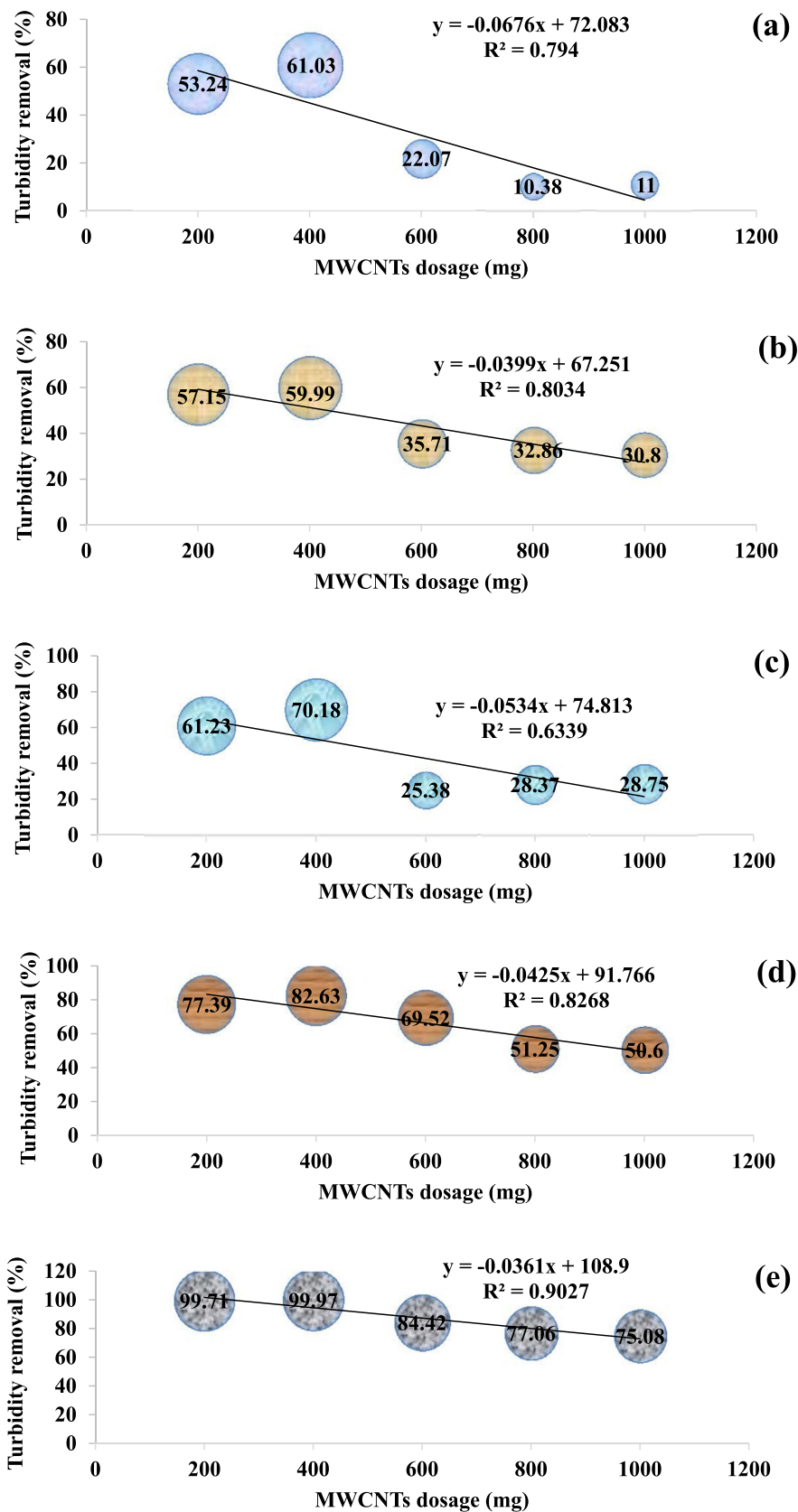


Fig. 11. Effect of MWCNTs growth (a) 700 °C (b) 750 °C (c) 800 °C (d) 850 °C (e) 900 °C on Turbidity removal.

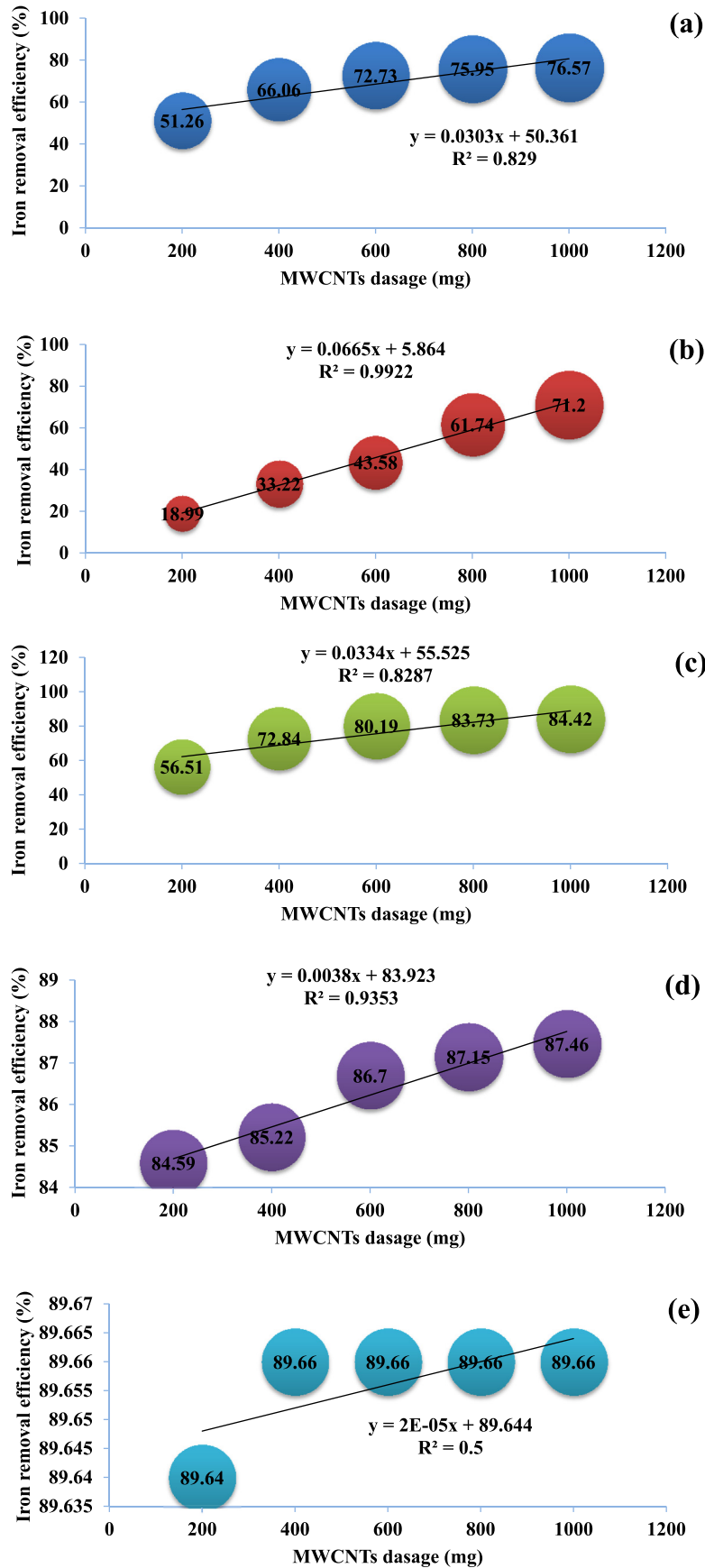


Fig. 12. Effect of MWCNTs growth (a) 700 °C (b) 750 °C (c) 800 °C (d) 850 °C (e) 900 °C on Iron (Fe) removal efficiency.

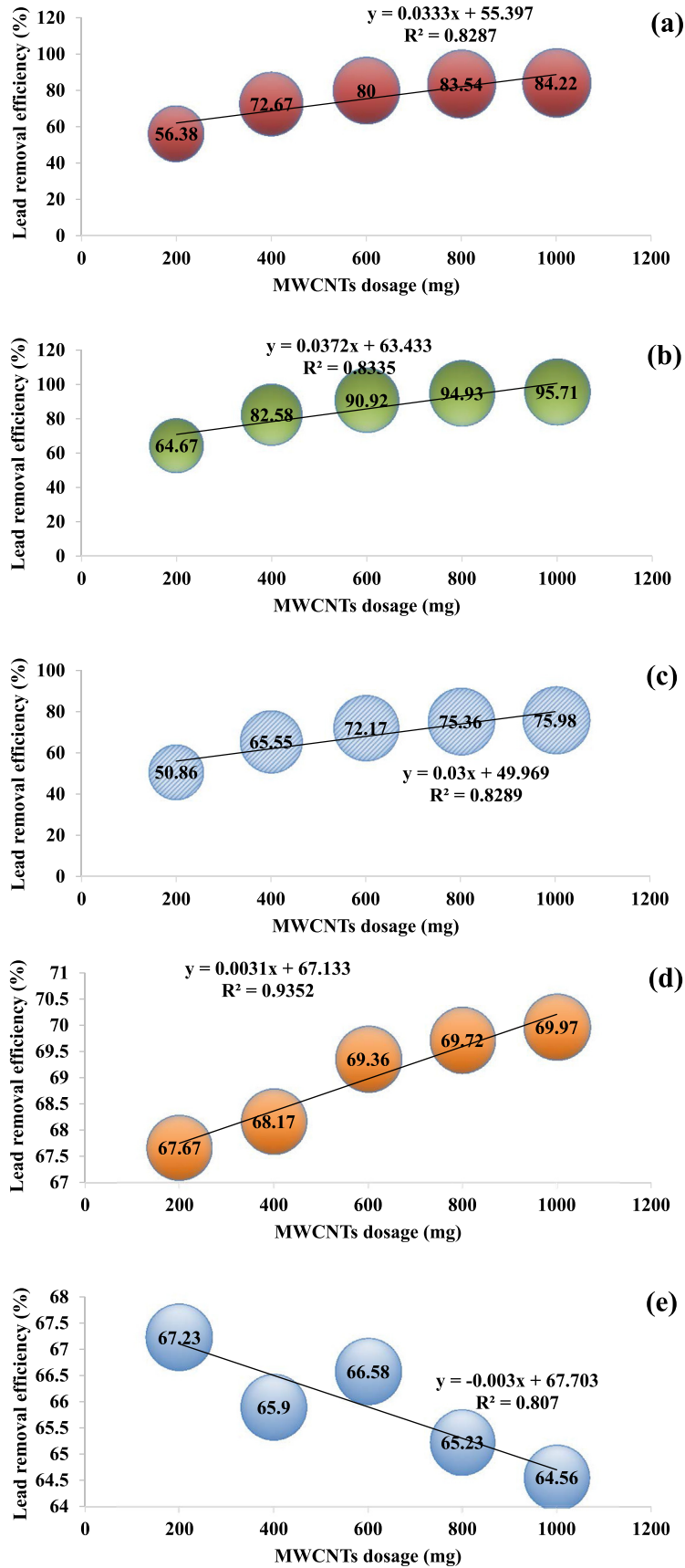


Fig. 13. Effect of MWCNTs growth (a) 700 °C (b) 750 °C (c) 800 °C (d) 850 °C (e) 900 °C on Lead (Pb) removal efficiency.

## Acknowledgements

Centre for Genetic Engineering and Biotechnology (CGEB) FUT-Minna is highly appreciated for having direct access to the centre's facilities.

## References

- Abdulrahman, M.A., Abubakre, O.K., Abdulkareem, S.A., Tijani, J.O., Aliyu, A., Afolabi, A.S., 2017. Effect of coating mild steel with CNTs on its mechanical properties and corrosion behaviour in acidic medium. *Adv. Nat. Sci. Nanosci. Nanotechnol.* **8**, 015016. <http://dx.doi.org/10.1088/2043-6254/aa5cf8>.
- Aliyu, A., Abdulkareem, A.S., Kovo, A.S., Abubakre, O.K., Tijani, J.O., Kariim, I., 2017. Synthesize multi-walled carbon nanotubes via catalytic chemical vapour deposition method on Fe-Ni bimetallic catalyst supported on kaolin. *Carbon Lett.* **21**, 33–50.
- Hutchison, J.L., Kiselev, N.A., Krinichnaya, E.P., Krestinin, A.V., Loutfy, R.O., Morawsky, A.P., 2001. Double-walled carbon nanotubes fabricated by a hydrogen arc discharge method. *Carbon* **39**, 761–770.
- Hayder, B.A., Irmawati, R., Ismayadi, I., Nor Azah, Y., 2017. Hydrocarbon sources for the carbon nanotubes production by chemical vapour deposition: a review. *Pertanika J. Sci. Technol.* **25** (2), 379–396.
- Iijima, S., 1991. Helical microtubules of graphitic carbon. *Nature* **354**, 56–58.
- Iijima, S., Ichihashi, T., 1993. Single-shell carbon nanotubes of 1-nm diameter. *Nature* **363**, 603–605.
- Kariim, I., Abdulkareem, A.S., Abubakre, O.K., Aliyu, A., Mohammed, I.A., Hamidu, A., 2017. Characterization and antibacterial activity of nickel ferrite doped  $\alpha$ -alumina nanoparticle. *Eng. Sci. Tech. Int. J.* **20** (2), 563–569.
- Kukovitsky, E.F., L'vov, S.G., Sainov, N.A., Shustov, V.A., Chernozatonskii, L.A., 2002. Correlation between metal catalyst particle size and carbon nanotube growth. *Chem. Phys. Lett.* **355**, 497.
- Maria, K.H., Mieno, T., 2015. Synthesis of single-walled carbon nanotubes by low frequency bipolar pulsed arc discharge method. *Vacuum* **113**, 11–18.
- Nair, N., Kim, W.J., Braatz, R.D., Strano, M.S., 2008. Dynamics of surfactant suspended single walled carbon nanotubes. *Langmuir* **24**, 1790–1795.
- Othman, C.S.A., Isaiah, O.A., Tawfik, A.S., 2017. Novel cross-linked melamine based polyamine/CNT composites for lead ions removal. *J. Environ. Manage.* **192**, 163–170.
- Shah, K.A., Tali, B.A., 2016. Synthesis of carbon nanotubes by catalytic chemical vapour deposition: a review on carbon sources, catalysts and substrates. *Mater. Sci. Semicond. Process* **41**, 67–82.
- Su, W., Zhu, Y., Zhang, J., Liu, Y., Yang, Y., Mao, Q., Li, L., 2016. Effect of multi-wall carbon nanotubes supported nano-nickel and TiF<sub>3</sub> addition on hydrogen storage properties of magnesium hydride. *J. Alloys Compd.* **669**, 8–18.
- Tasis, D., Tagmatarchis, N., Bianco, A., Prato, M., 2006. Chemistry of carbon nanotubes. *Chem. Rev.* **106**, 1105–1136.
- Tombros, N., Buit, L., Arfaoui, I., Tsoufis, T., Gournis, D., Trikalitis, P.N., 2008. Charge transport in a single superconducting tin nanowire encapsulated in a multi-walled carbon nanotube. *Nano Lett.* **8**, 3060–3064.
- Tsoufis, T., Jankovic, L., Gournis, D., Trikalitis, P.N., Bakas, T., 2008. Evaluation of first-row transition metal oxides supported on clay minerals for catalytic growth of carbon nanostructures. *Mater. Sci. Eng. B* **152**, 44–49.
- Voelskow, K., Becker, M.J., Xia, W., Muhler, M., Turek, T., 2014. The influence of kinetics, mass transfer and catalyst deactivation on the growth rate of multi-walled carbon nanotubes from ethane on a cobalt-based catalyst. *Chem. Eng. J.* **244**, 68–74.
- (WHO) WHO, 2011. World Health Organisation, Guidelines for Drinking Water Quality, fourth ed.
- Yang, H.Y., Han, Z.J., Yu, S.F., Pey, K.L., Ostrikov, K., Karnik, R., 2013. Carbon nanotubes for water desalination and purification. *Nat. Commun.* **4**, 2220.
- Yang, X., Zou, T., Shi, C., Lie, E., He, C., Zhao, N., 2016. Effect of carbon nanotube (CNT) content on the properties of in-situ synthesis CNT reinforced Al composites. *Mater. Sci. Eng. A* **660**, 11–18.
- Zhao, Q., Li, Y.H., Zhou, X.P., Jiang, T.S., Li, C.S., Yin, H.B., 2010. Synthesis of multi-wall carbon nanotubes by the pyrolysis of ethanol on Fe/MCM-41 mesoporous molecular sieves. *Superlattices Microstruct.* **47**, 432.